Multipole effects in atom-surface interactions: A theoretical study with an application to He–α-quartz

Grzegorz Łach,[1,*] Maarten DeKieviet,[1,†] and Ulrich D. Jentschura[2,‡]
[1]*Physikalisches Institut der Universität Heidelberg, Philosophenweg 12, 69120 Heidelberg, Germany*
[2]*Department of Physics, Missouri University of Science and Technology, Rolla, Missouri 65409-0640, USA*
(Received 14 January 2010; published 18 May 2010)

We address some practically important and experimentally relevant questions concerning atom-surface interactions. For example, the quadrupole interaction of an atom with a dielectric macroscopic surface is obtained with full allowance for retardation and in closed form, valid for an arbitrary atom-surface distance. We also explore the relevance of higher-order multipole effects in atom-surface interactions, and we find that details in the dielectric response function of the surface material have to be resolved in order to accurately calculate the atom-surface potential. They lead to important effects at an intermediate range which cannot be explained by either short-range or long-range asymptotics. A numerical example (helium interacting with α-quartz) is included in order to illustrate this aspect.

DOI: 10.1103/PhysRevA.81.052507 PACS number(s): 31.30.jh, 12.20.Ds, 31.15.−p

I. INTRODUCTION

The purpose of this article is to report on some advances in our theoretical understanding of interactions of neutral atoms with surfaces mediated by virtual excitations of the quantized electromagnetic field. These are commonly referred to as Casimir-Polder interactions. Casimir-Polder (long-range) interactions of atoms and surfaces have been studied theoretically for a number of decades. It is well known that for an atom in contact with a perfect conductor, the result of Casimir and Polder [1] states that the z^{-3} near-field interaction mediated by the quantum fluctuations of the electromagnetic field asymptotically changes to a z^{-4} interaction for long distances. (Throughout this article, the atom-wall distance is denoted as z.)

Lifshitz [2] generalized the result of Casimir and Polder to the case of a nonperfect conductor, within the electric-dipole approximation for the electronic currents. However, the generalization of the result of Lifshitz to the quadrupole interaction had yet to be determined in closed form. In the current article we examine the interaction of an atom with a dielectric, valid for an arbitrary range of the atom-surface distance and with retardation effects included.

Another aspect whose importance is sometimes underestimated concerns the accurate calculation of the dielectric response function of the surface in contact with the atom. Indeed, it turns out that an accurate numerical representation of both the atomic properties and the surface are crucial for obtaining reliable results for the atom-surface interaction potentials. We study as a numerical example ground-state helium interacting with the (0001)-crystalline surface of α-quartz (z cut). This system is found to display an intermediate region of distances, in between the short-range and the long-range asymptotic limits, where its characteristic shape cannot be explained by either asymptotic form.

The current theoretical study is inspired by the ongoing development of a spin-echo apparatus for atom-surface studies at Heidelberg University [3–5]. During the past decades, He atom scattering has proven to be a very useful tool for the investigation of both the structure and the dynamics of and at surfaces. At thermal energies, this noble-gas particle interacts nondestructively and is chemically completely inert. Being so light, its de Broglie wavelength matches the typical lattice constant of solids, so that atom diffraction has been used to obtain the most precise information on the shape and periodicity of the repulsive tail of the potential. In addition, He atom scattering serves as a very sensitive, *in situ* probe for the characterization of the quality, roughness, and cleanliness of the two-dimensional surface. Detailed information on the substrate is an ideal starting point and necessary requirement for any accurate Casimir experiment.

The atomic beam spin-echo method combines the exclusive surface sensitivity of a cold beam of ^{3}He atoms with the high resolution of nuclear spin-echo experiments. This atom interferometry technique has demonstrated high resolving power in both space (0.01 Å–10 μm) and energy (in the range of a few meV down to 10 peV) in surface scattering experiments, determining the structure and dynamics of (quasi-) two-dimensional systems. In a first series of experiments on Casimir-Polder physics (a detailed account of the experiments is be given elsewhere), this apparatus was used to fully characterize each system at this level of precision, using the repulsive tail of the atom-wall interaction.

The attractive branch of the atom-surface interaction potential is investigated by measuring the quantum reflectivity of ^{3}He atoms. The region within the interaction potential in which quantum reflection takes place strongly depends on the kinetic energy of the incident particle. The center of this reflection region is situated at some distance where the kinetic energy equals the potential energy. By going to grazing angles of incidence, this energy can be reduced to very low values, thus shifting the region of quantum reflection to larger and larger distances z. Monitoring the ^{3}He quantum reflectivity as a function of incident perpendicular momentum, one can map out the potential near and away from the wall. It is described in detail in Ref. [5] how this method probes the z^{-3} near-field

*gel@physi.uni-heidelberg.de
†maarten@physi.uni-heidelberg.de
‡ulj@mst.edu

van der Waals region, the z^{-4} far-field Casimir-Polder region, and the transition region in between. Experimental data at the percent level of relative accuracy have been obtained for a variety of substrates (metals, semiconductors, and insulators). These results are to be confronted to the theoretical full interaction potential, which can be calculated for many of these systems from (optical) data available in the literature [6].

With this experiment, we have arrived at a level of precision where this quantitative comparison forms a critical test of the model underlying these calculations and may for the first time reveal the need for including higher-order corrections. In this article, we primarily focus on the theoretical aspects of the problem; the connection to the spin-echo signal will be explored in more detail elsewhere. In Sec. II, basic formulas regarding multipole interactions are recalled. We then proceed to analyze the atom-wall interaction, starting with the case of a perfect conductor, in Sec. III. We attempt to describe the derivations in some detail. The asymptotic limits for short-range interactions, still with a perfect conductor, are explored in Sec. IV. The generalization of the results derived in Sec. III to the case of a dielectric are discussed in Sec. V, with full allowance for retardation effects. Finally, the general formulas obtained hitherto are applied to the case of the He–α-quartz interaction in Sec. VI. We conclude with a summary in Sec. VII.

The subject of this article is interesting for two communities: the quantum electrodynamics (QED) community and the atomic physics community. Atomic units with $|e| = \hbar = m = 1$ (where $|e|$ is the positive elementary charge unit and m is the electron mass) are contrasted with natural units where $\hbar = c = \epsilon_0 = 1$ and $e^2 = 4\pi\alpha$. In order to "interpolate" between the two communities, we use a different system of units here, namely, the Système International (SI). The length of the formulas is not drastically altered by the use of the SI, as intermediate expressions do not display excessive complexity, and the use of the SI, apart from being recommended by CODATA [7], also enables the direct evaluation of formulas for experimental purposes.

II. MULTIPOLE INTERACTIONS

The authors of Ref. [8] provide for very consistent definitions of multipole polarizabilities of atoms, and since these are important for the current study, we briefly recall their conventions. From Eq. (6) of Ref. [8], we learn that the 2^L-pole dynamic polarizability α_L of the ground state $|\psi_0\rangle$ of an atom, the oscillator strength $f_{n0}^{(l)}$, and the energy differences $E_{n0} = E_n - E_0$ of a virtual excited state $|\Psi_n\rangle$ are related by

$$\alpha_L(\omega) = \sum_n \frac{f_{n0}^{(L)}}{E_{n0}^2 - (\hbar\omega)^2}, \tag{1}$$

where the sum over n also includes the continuous spectrum and the oscillator strength is

$$f_{n0}^{(L)} = \frac{8\pi e^2}{2L+1} E_{n0} \left| \langle \Psi_0 | \sum_i (r_i)^L Y_{Lm}(\hat{r}_i) | \Psi_n \rangle \right|^2, \tag{2}$$

and it is independent of m provided one sums over the magnetic projections of the excited state n. Here, $\vec{r}_i$ is the radial coordinate of the ith electron, and $Y_{Lm}(\hat{r}_i)$ is the spherical harmonic. The sum is over all electrons i at position $\vec{r}_i$ of the system. In view of the identity

$$\frac{2E_{n0}}{E_{n0}^2 - (\hbar\omega)^2} = \frac{1}{E_{n0} - \hbar\omega} + \frac{1}{E_{n0} + \hbar\omega}, \tag{3}$$

we can write $\alpha_L(\omega)$ as

$$\begin{aligned} &\alpha_L(\omega) \\ &= \frac{4\pi e^2}{2L+1} \sum_n \langle \Psi_0 | \sum_i (r_i)^L Y_{Lm}(\hat{r}_i) | \Psi_n \rangle \\ &\quad \times \langle \Psi_n | \sum_j (r_j)^L Y_{Lm}^*(\hat{r}_j) | \Psi_0 \rangle \left(\frac{1}{E_{n0} - \hbar\omega} + \frac{1}{E_{n0} + \hbar\omega} \right) \\ &= \langle \Psi_0 | Q_{Lm} \left(\frac{1}{H - E_0 - \hbar\omega} + \frac{1}{H - E_0 + \hbar\omega} \right) Q_{Lm}^* | \Psi_0 \rangle, \end{aligned} \tag{4}$$

where

$$Q_{Lm} = e\sqrt{\frac{4\pi}{2L+1}} \sum_i (r_i)^L Y_{Lm}(\hat{r}_i), \tag{5a}$$

$$Q_{Lm}^* = (-1)^m e\sqrt{\frac{4\pi}{2L+1}} \sum_i (r_i)^L Y_{L-m}(\hat{r}_i). \tag{5b}$$

Here, the sum over n extends over the complete spectrum, and it includes, in particular, all magnetic projections of the virtual states $|\Psi_n\rangle$.

We now turn our attention to the question how the multipole polarizabilities affect the energy of the atom in the presence of an electric field. For the atom-wall interaction, which is mediated primarily by electromagnetic waves with a wavelength that is long compared to the dimensions of the atoms, we can use the effective long-wavelength Hamiltonian governing the interaction [9]. For the electric field, we can thus use the expansion

$$\begin{aligned} H_I = &-e r^i E^i - \frac{e}{2} r^i r^j \nabla^j E^i - \frac{e}{6} r^i r^j r^k \nabla^j \nabla^k E^i \\ &- \frac{e}{4!} r^i r^j r^k r^l \nabla^j \nabla^k \nabla^l E^i. \end{aligned} \tag{6}$$

For the dipole contribution to the atom-wall interaction, we have

$$\mathcal{E}_1 = -\frac{1}{2} \sum_{\vec{k}\lambda} \alpha_1(\omega) |\vec{E}_{\vec{k}\lambda}(\vec{r})|^2, \tag{7}$$

where $\vec{E}_{\vec{k}\lambda}(\vec{r})$ is the electric field corresponding to the field mode with wave vector $\vec{k}$ and polarization λ. Based on the definition of the multipole polarizability in Eq. (4), we have for the quadrupole term

$$\mathcal{E}_2 = -\frac{1}{12} \sum_{\vec{k}\lambda} \sum_{ij} \alpha_2(\omega) \left| \nabla^j E_{\vec{k}\lambda}^i(\vec{r}) \right|^2, \tag{8}$$

where we reserve the index i for the component of the electric field. The octupole energy shift, by contrast, is

$$\mathcal{E}_3 = -\frac{1}{180}\sum_{\vec{k}\lambda}\sum_{ijk}\alpha_3(\omega)\left|\nabla^j\nabla^k E^i_{\vec{k}\lambda}(\vec{r})\right|^2, \tag{9}$$

and for the hexadecupole energy shift, we obtain

$$\mathcal{E}_4 = -\frac{1}{5040}\sum_{\vec{k}\lambda}\sum_{ijkl}\alpha_4(\omega)\left|\nabla^j\nabla^k\nabla^l E^i_{\vec{k}\lambda}(\vec{r})\right|^2. \tag{10}$$

The generalization to a 2^L-pole polarizability is found to be

$$\mathcal{E}_L = -\frac{2^{L-1}}{(2L)!}\sum_{\vec{k}\lambda}\sum_{j_1 j_2\cdots j_L}\sum_{i}\alpha_L(\omega)\left|\nabla^{j_1}\nabla^{j_2}\cdots\nabla^{j_L}E^i_{\vec{k}\lambda}(\vec{r})\right|^2. \tag{11}$$

III. PERFECT CONDUCTOR, ARBITRARY RANGE

For the description of the atom-wall interaction, we have to assume the atom being immersed in a superposition of incoming and reflected waves (from the surface). The surface is assumed to lie in the xy plane (i.e., at $z = 0$), and we initially assume boundary conditions for a waveguide extending from $x = 0$ to $x = L$ and $y = 0$ to $y = L$, and we assume the atom to be at a distance z from the surface. The procedure then is to evaluate the interaction energy according to formulas (7)–(10) with the aforementioned waveguide modes in place, for an atom at point $\vec{r} = (\frac{1}{2}L, \frac{1}{2}L, z)$, and then, to average over x and y. In the next step of the calculation, a z-independent constant is identified as a renormalization term ("mass counter term"), which represents an additional renormalization of the mass (energy) of the bound system in the presence of the atom-wall interaction mediated by the modes. Alternatively, one may say that the renormalization ensures that as $z \to \infty$, the atom experiences a zero energy shift due to the distant wall, which is physically reasonable. This procedure implies both a subtraction of the constant term and also a regularization of the remaining integral, which is oscillating in the z direction, by a convergent factor $\exp(-\epsilon z)$. We can alternatively implement the convergent factor as a Wick rotation of the photon energy integration. Finally, we obtain a finite interaction energy.

We follow pages 261–263 of Ref. [10] and discuss the mode structure for finite dielectric constant. In the current section, we always take the perfect conductor limit

$$\varepsilon(\omega) \to \infty \tag{12}$$

before coming back to the full discussion of the dielectric in Sec. VII. The wave vectors of the modes (perpendicular component $\vec{k}_\perp$ and reflected component $\vec{k}^{\rm R}$) are denoted as

$$\vec{k} = (k_1, k_2, k_3), \quad \vec{k}_\perp = (k_1, k_2, 0), \tag{13a}$$

$$\vec{k}^{\rm R} = (k_1, k_2, -k_3) = 2\vec{k}_\perp - \vec{k}. \tag{13b}$$

In describing the reflection from the boundary, we notice that the index of refraction $n(\omega)$ is usually connected with the change in the speed of light in the medium according to $c \to c/n(\omega)$, where we have $n(\omega) = \sqrt{\varepsilon(\omega)}$. We always assume a material whose magnetic permeability is equal to that of the vacuum. In the absence of absorptive effects, the frequency of the light does not change in the transition toward the medium; the wavelength in general becomes shorter, so that the k wave vector becomes $k' > k$,

$$\frac{c}{n(\omega)} = \frac{\omega}{k'}, \quad n(\omega) = \sqrt{\varepsilon(\omega)}, \tag{14}$$

$$k' = \sqrt{\varepsilon(\omega)}k = \sqrt{\varepsilon(\omega)}\frac{\omega}{c}. \tag{15}$$

In the case of a perfect conductor,

$$\varepsilon(\omega) \to \infty, \quad k' \to \infty, \tag{16}$$

which means that no electromagnetic wave can enter into a perfect conductor. To summarize, the z components of the wave vectors of the incoming and reflected waves can be written as follows:

$$k_3 = \sqrt{\frac{\omega^2}{c^2} - k_1^2 - k_2^2}, \quad k_3' = \sqrt{\varepsilon(\omega)\frac{\omega^2}{c^2} - k_1^2 - k_2^2}. \tag{17}$$

Under the aforementioned boundary conditions for a waveguide, the transverse electric (TE) and transverse magnetic (TM) modes correspond to those for a waveguide directed along the z axis, with boundary conditions in the x and y directions. These modes have been illustrated in the literature on various occasions (e.g., in Refs. [11,12]). The incoming (index I) TE- and TM-mode electromagnetic waves are given as

$$\vec{A}^{\rm I,TE}_{\vec{k}\lambda} \equiv \sqrt{\frac{\hbar c^2}{2\epsilon_0\omega_k V}}\vec{\epsilon}_{\vec{k}\lambda}e^{i\vec{k}\cdot\vec{r}}, \tag{18a}$$

$$\vec{A}^{\rm I,TM}_{\vec{k}\lambda} \equiv \sqrt{\frac{\hbar c^2}{2\epsilon_0\omega_k V}}\left(\vec{\epsilon}_{\vec{k}\lambda}\times\frac{\vec{k}}{k}\right)e^{i\vec{k}\cdot\vec{r}}. \tag{18b}$$

The reflected waves (index R) are given by

$$\vec{A}^{\rm R,TE}_{\vec{k}\lambda} = \sqrt{\frac{\hbar c^2}{2\epsilon_0\omega_k V}}\vec{\epsilon}_{\vec{k}\lambda}\frac{k_3 - k_3'}{k_3 + k_3'}e^{i\vec{k}^{\rm R}\cdot\vec{r}}, \tag{19a}$$

$$\vec{A}^{\rm R,TM}_{\vec{k}\lambda} = \sqrt{\frac{\hbar c^2}{2\epsilon_0\omega_k V}}\left(\vec{\epsilon}_{\vec{k}\lambda}\times\frac{\vec{k}^{\rm R}}{k}\right)\frac{\varepsilon(\omega)k_3 - k_3'}{\varepsilon(\omega)k_3 + k_3'}e^{i\vec{k}^{\rm R}\cdot\vec{r}}. \tag{19b}$$

For a perfect conductor, we have

$$\vec{A}^{\rm R,TE}_{\vec{k}\lambda} = -\sqrt{\frac{\hbar c^2}{2\epsilon_0\omega_k V}}\vec{\epsilon}_{\lambda\vec{k}}e^{i\vec{k}^{\rm R}\cdot\vec{r}}, \tag{20a}$$

$$\vec{A}^{\rm R,TM}_{\vec{k}\lambda} = \sqrt{\frac{\hbar c^2}{2\epsilon_0\omega_k V}}\left(\vec{\epsilon}_{\lambda\vec{k}}\times\frac{\vec{k}^{\rm R}}{k}\right)e^{i\vec{k}^{\rm R}\cdot\vec{r}}. \tag{20b}$$

We here use the conventions of Ref. [10], but we convert the expressions to SI units (in Ref. [10], the Gaussian system is used).

The total vector potentials from superimposed incoming and reflected waves are thus given by

$$\vec{A}^{\rm TE}_{\vec{k}\lambda} = \sqrt{\frac{\hbar c^2}{2\epsilon_0\omega_k V}}\vec{\epsilon}_{\lambda\vec{k}}\left(e^{i\vec{k}\cdot\vec{r}} - e^{i\vec{k}^{\rm R}\cdot\vec{r}}\right)$$

$$= \sqrt{\frac{\hbar c^2}{2\epsilon_0\omega_k V}}\vec{\epsilon}_{\lambda\vec{k}}2i\sin(k_3 z)e^{i\vec{k}_\perp\cdot\vec{r}}, \tag{21a}$$

$$\vec{A}^{\rm TM}_{\vec{k}\lambda} = \sqrt{\frac{\hbar c^2}{2\epsilon_0\omega_k V}}\left[\left(\vec{\epsilon}_{\lambda\vec{k}}\times\frac{\vec{k}}{k}\right)(e^{ik_3z}-e^{-ik_3z}) + 2\left(\vec{\epsilon}_{\vec{k}\lambda}\times\frac{\vec{k}_\perp}{k}\right)e^{-ik_3z}\right]e^{i\vec{k}_\perp\cdot\vec{r}}. \tag{21b}$$

For both the TE and the TM modes, the x and y components of these vector potentials vanish on the perfectly conducting plate, that is, at $z=0$. This is immediately clear for the term $\sin(k_3z)$ that is relevant to the TE modes. For the term with the TM modes, this is also clear for the term proportional to $e^{ik_3z}-e^{-ik_3z}$. It is less clear for the term proportional to $\vec{\epsilon}_{\lambda\vec{k}}\times\vec{k}_\perp$. However, since $\vec{k}_\perp$ lies in the plane of the perfect conductor, it is immediately clear that $\vec{\epsilon}_{\lambda\vec{k}}\times\vec{k}_\perp$ points out of the xy plane.

The (z-dependent part of the) energy of a dipole polarizable particle reads (see Eq. (7) and Ref. [10])

$$\mathcal{E}_1(z) = -\frac{1}{2}\sum_{\vec{k}\lambda}\alpha_1(\omega_k)|\vec{E}_{\vec{k}\lambda}(z)|^2 = -\frac{1}{2}\sum_{\vec{k}\lambda}\alpha_1(\omega_k)\frac{\omega_k^2}{c^2}|\vec{A}_{\vec{k}\lambda}(z)|^2, \tag{22}$$

with $\vec{A}_{\vec{k}\lambda}$ being a sum of potentials from TE and TM modes,

$$\vec{A}_{\vec{k}\lambda} = \vec{A}^{\rm TE}_{\vec{k}\lambda} + \vec{A}^{\rm TM}_{\vec{k}\lambda}. \tag{23}$$

We here suppress the dependence of $\vec{A}_{\vec{k}\lambda}$ on the x and y coordinates and imply an averaging over x and y. The remaining z dependence is indicated in Eq. (22). The preceding formula can be conveniently simplified by the use of the following identity for polarizations sums,

$$\sum_\lambda(\vec{\epsilon}_{\lambda\vec{k}}\times\vec{a})\cdot(\vec{\epsilon}_{\lambda\vec{k}}\times\vec{b}) = \left(\delta^{ij}+\frac{k^ik^j}{k^2}\right)a^ib^j. \tag{24}$$

The interference term between TE and TM waves vanish, and after averaging over x and y, one obtains

$$\sum_\lambda\left|\vec{A}^{\rm TE}_{\vec{k}\lambda}(z)\right|^2 = \frac{2\hbar c^2}{\epsilon_0\omega_k V}\sin^2(k_3z) = -\frac{\hbar c^2}{\epsilon_0\omega_k V}\cos(2k_3z)+C, \tag{25a}$$

$$\sum_\lambda\left|\vec{A}^{\rm TM}_{\vec{k}\lambda}(z)\right|^2 = -\frac{\hbar c^2}{\epsilon_0\omega_k V}\left(1-2\frac{k_\perp^2}{k^2}\right)\cos(2k_3z)+C', \tag{25b}$$

where C and C' are z-independent constants. We make a corresponding substitution in Eq. (22) and take into account the fact that we should only have two polarization vectors per propagation vector. Then, the dipole energy $\mathcal{E}_1(z)$ evaluates to

$$\mathcal{E}_1(z) = -\frac{1}{4\epsilon_0}\sum_{\vec{k}\lambda}\alpha_1(\omega_k)\frac{\omega_k^2}{c^2}\left[\left|\vec{A}^{\rm TE}_{\vec{k}\lambda}(z)\right|^2+\left|\vec{A}^{\rm TM}_{\vec{k}\lambda}(z)\right|^2\right] = \frac{1}{2\epsilon_0 V}\sum_{\vec{k}\lambda}\alpha_1(\omega_k)(\hbar\omega_k)\left(1-\frac{k_\perp^2}{k^2}\right)\cos(2k_3z), \tag{26}$$

which in the continuum limit is equal to

$$\begin{aligned}\mathcal{E}_1(z) &= \frac{1}{2\epsilon_0 V}\frac{V}{(2\pi)^3}\int_0^\infty dk_3\int d^2\vec{k}_\perp \times\alpha_1(\omega_k)(\hbar\omega_k)\left(1-\frac{k_\perp^2}{k^2}\right)\cos(2k_3z)\\ &= \frac{\hbar c}{8\pi^2\epsilon_0}\int_0^\infty dk k^3\alpha_1(ck)\times\int_0^\pi d\theta\sin\theta\cos^2\theta\cos(2zk\cos\theta).\end{aligned}$$

We now introduce a convergent factor, which amounts to a Wick rotation of the integration contour, and change the interaction from k to ω. Finally, we arrive at the formula

$$\mathcal{E}_1(z) = -\frac{\hbar}{(4\pi)^2\epsilon_0 z^3}\int_0^\infty d\omega\,\alpha_1(i\omega)\times\left[1+\frac{2\omega z}{c}+2\left(\frac{\omega z}{c}\right)^2\right]e^{-2\omega z/c}. \tag{27}$$

This formula is in agreement with the literature (see Refs. [1,13,14]). It interpolates between the short-range z^{-3} asymptotics and the large-distance z^{-4} asymptotics. The short-range limit is

$$\mathcal{E}_1(z)\stackrel{z\to0}{=}-\frac{\hbar}{(4\pi)^2\epsilon_0 z^3}\int_0^\infty d\omega\,\alpha_1(i\omega), \tag{28}$$

and the large-distance limit is found as

$$\mathcal{E}_1(z)\stackrel{z\to\infty}{=}-\frac{3\hbar c\alpha_1(0)}{32\pi^2\epsilon_0 z^4} = -\frac{3}{8z^4}\frac{\alpha}{\pi}\frac{(\hbar c)^2}{e^2}\alpha_1(0). \tag{29}$$

The second form on the right-hand side very clearly displays the physics: We are talking about a second-order energy perturbation which is proportional to the QED coupling parameter α/π, where α is the fine-structure constant. The dimension of $\hbar c$ is that of energy times length, and together with the dipole operators in the scaled polarizability $\alpha_1(0)/e^2$ we obtain the square of the energy and the fourth power of length. The four powers of length are compensated by the $1/z^4$ factor, and one power of the energy is compensated by the propagator denominator in the polarizability. The result is an interaction energy, namely, $\mathcal{E}_1(z)$.

For the following formulas which are related to multipole and generalized polarizabilities, we have to take into account the fact that the higher-order multipoles generate additional factors of the coordinate in the numerator, which are in turn compensated by additional factors of z in the denominator. The quadrupole contribution to the atom-surface interaction has been investigated in Refs. [15–17]. According to Eq. (8), the energy of a quadrupole polarizable particle in a nonuniform electric field is equal to

$$\mathcal{E}_2(z) = -\frac{1}{12}\sum_{\vec{k}\lambda,ij}\alpha_2(\omega_k)\frac{\omega_k^2}{c^2}\left|\nabla^jA^i_{\vec{k}\lambda}(z)\right|^2. \tag{30}$$

The electric field gradients for the TE modes are equal to

$$\nabla^jA^{i,{\rm TE}}_{\vec{k}\lambda} = c\sqrt{\frac{\hbar}{2\epsilon_0\omega_k V}}2i\epsilon^i_{\lambda\vec{k}}[k^j\cos(k_3z)-k_\perp^je^{-ik_3z}]e^{i\vec{k}_\perp\cdot\vec{r}}. \tag{31}$$

After an analogous calculation for the TM modes, substitution to Eq. (30), and some simplification, we find

$$\mathcal{E}_2(z) = -\frac{\hbar}{(4\pi)^2\epsilon_0 z^5}\int_0^\infty d\omega\,\alpha_2(i\omega)e^{-2\omega z/c} \times\left[1+2\frac{\omega z}{c}+\frac{11}{6}\left(\frac{\omega z}{c}\right)^2+\left(\frac{\omega z}{c}\right)^3+\frac{1}{3}\left(\frac{\omega z}{c}\right)^4\right]. \tag{32}$$

In the short-range limit, we recover the result from Ref. [17],

$$\mathcal{E}_2(z)\overset{z\to 0}{=}-\frac{\hbar}{(4\pi)^2\epsilon_0 z^5}\int_0^\infty d\omega\,\alpha_2(i\omega). \tag{33}$$

In large-distance limit,

$$\mathcal{E}_2(z)\overset{z\to\infty}{=}-\frac{25\hbar c\alpha_2(0)}{192\pi^2\epsilon_0 z^6}=-\frac{25}{48z^6}\frac{\alpha}{\pi}\frac{(\hbar c)^2}{e^2}\alpha_2(0). \tag{34}$$

With the help of computer algebra [18], these results can be generalized to the octupole and hexadecupole interactions as follows. We start with the octupole,

$$\mathcal{E}_3(z) = -\frac{\hbar}{(4\pi)^2\epsilon_0 z^7}\int_0^\infty d\omega\,\alpha_3(i\omega)e^{-2\omega z/c} \times\left[1+2\frac{\omega z}{c}+\frac{28}{15}\left(\frac{\omega z}{c}\right)^2+\frac{16}{15}\left(\frac{\omega z}{c}\right)^3 +\frac{37}{90}\left(\frac{\omega z}{c}\right)^4+\frac{1}{9}\left(\frac{\omega z}{c}\right)^5+\frac{1}{45}\left(\frac{\omega z}{c}\right)^6\right]. \tag{35}$$

The short-range limit is

$$\mathcal{E}_3(z)\overset{z\to 0}{=}-\frac{\hbar}{(4\pi)^2\epsilon_0 z^7}\int_0^\infty d\omega\,\alpha_3(i\omega), \tag{36}$$

and we find the large-distance asymptotics

$$\mathcal{E}_3(z)\overset{z\to\infty}{=}-\frac{301\hbar c\alpha_3(0)}{1920\pi^2\epsilon_0 z^8}=-\frac{301}{480z^8}\frac{\alpha}{\pi}\frac{(\hbar c)^2}{e^2}\alpha_3(0). \tag{37}$$

The hexadecupole results are as follows,

$$\mathcal{E}_4(z) = -\frac{\hbar}{(4\pi)^2\epsilon_0 z^9}\int_0^\infty d\omega\,\alpha_3(i\omega)e^{-2\omega z/c} \times\left[1+2\frac{\omega z}{c}+\frac{53}{28}\left(\frac{\omega z}{c}\right)^2+\frac{47}{42}\left(\frac{\omega z}{c}\right)^3 +\frac{193}{420}\left(\frac{\omega z}{c}\right)^4+\frac{29}{210}\left(\frac{\omega z}{c}\right)^5+\frac{79}{2520}\left(\frac{\omega z}{c}\right)^6 +\frac{1}{180}\left(\frac{\omega z}{c}\right)^7+\frac{1}{1260}\left(\frac{\omega z}{c}\right)^8\right]. \tag{38}$$

In the short-range limit, we recover a meanwhile familiar prefactor,

$$\mathcal{E}_4(z)\overset{z\to 0}{=}-\frac{\hbar}{(4\pi)^2\epsilon_0 z^9}\int_0^\infty d\omega\,\alpha_4(i\omega), \tag{39}$$

whereas the large-distance limit is

$$\mathcal{E}_4(z)\overset{z\to\infty}{=}-\frac{1593\,\hbar c\,\alpha_4(0)}{8960\pi^2\epsilon_0 z^{10}}=-\frac{1593}{2240\,z^{10}}\frac{\alpha}{\pi}\frac{(\hbar c)^2}{e^2}\alpha_4(0). \tag{40}$$

We note that the numerical, rational prefactors in Eqs. (29), (34), and (37) are numerically close to 3/8, 4/8, and 5/8, respectively, whereas the rational prefactor in Eq. (40) departs from the "prediction" 6/8. The physical process under study is too complicated in order for the linear extrapolation to be reliable. We have verified the prefactor 1593/2240 in Eq. (40) by an independent calculation based on Chapter 3 of Ref. [10], where an approach is described which is valid only for the large-distance asymptotics in the dipole approximation. An obvious generalization of the latter approach to the case of the hexadecupole polarizability then confirms the aforementioned prefactor.

IV. PERFECT CONDUCTOR, SHORT RANGE

A. General asymptotic considerations

It is useful, for later considerations, to consider the asymptotic limits of large and small separation of the atom from the wall. In order to fix ideas, we should remember that the subject of this article concerns interactions of an atom and a flat surface at low temperature (we do not consider corrugated surfaces, and temperature-induced effects are also excluded from the discussion). Under these conditions, there are two scales in the problem, the Bohr radius,

$$a_0=\frac{\hbar}{\alpha mc}, \tag{41}$$

and the wavelength of a typical atomic transition,

$$\lambda\!\!\!^{-}_0=\frac{\hbar}{\alpha^2 mc}=\alpha^{-1}a_0. \tag{42}$$

The latter is the scale at which the retardation of electromagnetic interactions become important and separates the short- and long-range regimes.

A priori, the short-range regime for the atom-wall interaction is given by the condition

$$a_0 \ll z \ll \lambda\!\!\!^{-}_0, \tag{43}$$

where the atom-wall distance z is much larger than the Bohr radius, in order to prevent any overlap of the atomic wave function with the substrate. However, the condition $z \gg a_0$ should be taken *cum grano salis* ("with a grain of salt") and, indeed, stricter conditions must sometimes be used. These have their origin in phenomenological considerations [19–23]. First of all, in the case of any appreciable overlap of the atomic wave function with the substrate (even if exponentially suppressed), one should use so-called damping functions (see Ref. [21] and references therein) in order to describe the deviations from the van der Waals law. Indeed, the damping functions, which can be parameterized in terms of Fermi distribution type functions, model the deviation from the near-field asymptotics of the van der Waals interaction. For atoms and molecules, this interaction is of the form $1/R^6$ in the interatomic separation R, and it is of the form $1/z^3$ in the atom-wall distance z. Deviations from this form for close approach are modeled by the "damping functions."

The limit for close approach when the van der Waals interaction breaks down should be investigated very carefully also for a second reason. We have made the assumption that only two interactions with the quantized electromagnetic field take place, and our expressions are of first order in the multipole polarizabilities. In Refs. [19,20,22,23], it is pointed out that for close approach, higher-order (in the dipole polarizability α_1) energy shifts may become important. The

parameter governing this expansion, in SI units, reads (see Eq. (2.28) of Ref. [22])

$$\gamma = \alpha \frac{\hbar c \alpha_1(\omega)}{z^3}, \tag{44}$$

and our approximation of taking only the first term in the expansion in γ requires that $\gamma \ll 1$. The full correction is obtained after an integral involving $\gamma = \gamma(\omega)$ (see Eq. (6.1) of Ref. [23]). Generally, atomic wavelengths $\lambda\!\!\!^{-}_0$ are larger than the Bohr radius by a factor α^{-1} [see Eq. (42)], and they are also larger than the closest approach of atom and wall in many typical experiments. When even the parameter $\gamma' = \alpha \hbar c \alpha_1(\omega)/\lambda\!\!\!^{-3}_0$ fails to fulfill $\gamma' \ll 1$, then it becomes indispensable to consider the higher-order effects in the polarizability at a general atom-wall distance. Finally, we should point out that all statements and order-of-magnitude estimates are subject to adjustment for a particular atom. For example, for atoms in their ground state, $\alpha_1(0)$ typically is of order one (in atomic units). In some cases, however, for example, for Rydberg states, it can be orders of magnitude greater. This concludes our discussion on possible additional restrictions clarifying the condition $z \gg a_0$, which limits the short-distance regime from below.

The large-distance regime on the other hand, is given by

$$z \gg \lambda\!\!\!^{-}_0 \gg \left(\frac{\alpha_1(0)}{4\pi\epsilon_0}\right)^{1/3} \gtrsim a_0. \tag{45}$$

The multipole expansion generates higher powers of the atomic coordinate r in view of the structure of Eq. (2), which are compensated by more and more powers of the atom-wall distance z in the denominator of the energy shifts. The expansion into multipoles, therefore, is an expansion in powers of the parameter

$$\xi = \frac{a_0}{z} = \frac{\hbar}{\alpha m z c} \ll 1, \tag{46}$$

which is less than unity for both ranges (43) and (45) indicated above, but not necessarily very small if the atom is close to the wall. Therefore, a consideration of multipole corrections becomes important for close approach.

In the short-range limit, a second expansion is possible. Namely, the polynomials in $\omega z/c$ which are present in Eqs. (27), (32), (35), and (38), generate an expansion in ascending powers of

$$\zeta = \frac{\alpha^2 m z c}{\hbar} = \frac{\alpha}{\xi}, \tag{47}$$

which is a small parameter ($\ll 1$) for the short-range regime (43).

For the large-distance limit, the situation is completely different. Here, we may expand the polarizability for small argument, $\alpha_L(i\omega) = \alpha_L(0) + \omega^2 \beta_L(0) + \cdots$. In view of the exponential factor $\exp(-\omega z/c)$, this is an expansion in powers of

$$\frac{1}{\zeta} = \frac{c}{z}\frac{\hbar}{\alpha^2 m c^2} = \frac{\hbar}{\alpha^2 m z c}. \tag{48}$$

This parameter is small only in the large-distance regime (45). The applicability of the latter expansion has already been mentioned in Ref. [24].

Furthermore, because the large-distance limit of all multipole interactions entails one more inverse power of z than the short-range limit, it is natural to sum the ascending powers of ζ which multiply the short-range asymptotics by a Padé approximant in z with a denominator degree exceeding the numerator degree by one. However, before we use this observation in Sec. VI, we first discuss an anomaly which plagues the expansion in ascending powers of ζ for the short-range regime.

B. Dipole and quadrupole with correction term

The short-range asymptotics for the dipole, quadrupole, and octupole polarizabilities have been recorded in Eqs. (28), (33), (36), and (39). The general form, for a 2^L-pole polarizability, is

$$\mathcal{E}_L(z) = -\frac{\hbar}{(4\pi)^2 \epsilon_0 z^{2L+1}} \int_0^\infty d\omega\, \alpha_L(i\omega). \tag{49}$$

This is the leading term in the expansion for small z of the atom-surface interaction. However, there are correction terms corresponding to an expansion in ascending powers of the parameter $\zeta = \alpha^2 m z c/\hbar$ as defined in Eq. (47). The next-to-leading order in this expansion would lead to a divergent integral of the form $\int_0^\infty d\omega \omega^2 \alpha_L(i\omega)$. We here observe that the linear term in the expansion in $\omega z/c$ cancels between the polynomial and exponential terms in the integrand on the right-hand side of Eq. (27). The quadratic term, for a perfect conductor, then gives rise to the aforementioned integral which diverges for large frequencies. We see in Sec. V that the divergence can be avoided for a realistic conductor, because of general properties of the dielectric response function in the ultraviolet, but it is still interesting and necessary to clarify the treatment of the divergence within the approximation of a perfect conductor.

To this end, we observe that the dynamic polarizability can be written in the form [see Eq. (1)]

$$\hbar^2 \alpha_L(i\omega) = \sum_n \frac{f_{n0}^{(L)}}{\omega_{n0}^2 + \omega^2}, \tag{50}$$

where the f_{n0} are the oscillator strengths given in Eq. (2). In order to solve the problem, one has to perform the integral over ω without any approximations,

$$\begin{aligned} I_n(\mu) &= \int_0^\infty d\omega \frac{e^{-\omega\mu}}{\omega_{n0}^2 + \omega^2} \\ &= \frac{1}{\omega_{n0}}[\sin(\mu\omega_{n0})\mathrm{Ci}(\mu\omega_{n0}) - \cos(\mu\omega_{n0})\mathrm{si}(\mu\omega_{n0})], \end{aligned} \tag{51}$$

where the $\mathrm{Ci}(x)$ and $\mathrm{si}(x)$ are the cosine and sine integrals,

$$\mathrm{Ci}(x) = -\int_x^\infty \frac{\cos t}{t} dt, \quad \mathrm{si}(x) = -\int_x^\infty \frac{\sin t}{t} dt. \tag{52}$$

We here use the standard definitions (see Eqs. (5.2.1), (5.2.2), (5.2.5), (5.2.26), and (5.2.27) in Ref. [25]) for the cosine integral Ci and the sine integral si. The exact results for the

dipole and quadrupole energies can then be written in terms of parametric differentiations of the integral $I_n(\mu)$,

$$\hbar^2\mathcal{E}_1(z) = -\frac{\hbar}{(4\pi)^2\epsilon_0 z^3}\sum_n \left|f_{n0}^{(1)}\right|^2\left[1+2(-\mu)\frac{\partial}{\partial\mu} + 2(-\mu)^2\frac{\partial^2}{\partial\mu^2}\right] I_n(\mu)\Big|_{\mu=2z/c}. \tag{53}$$

For the quadrupole shift, we obtain

$$\hbar^2\mathcal{E}_2(z) = -\frac{\hbar}{(4\pi)^2\epsilon_0 z^5}\sum_n \left|f_{n0}^{(2)}\right|^2\left[1-2\mu\frac{\partial}{\partial\mu}+\frac{11}{6}\mu^2\frac{\partial^2}{\partial\mu^2} - \mu^3\frac{\partial^3}{\partial\mu^3}+\frac{1}{3}\mu^4\frac{\partial^4}{\partial\mu^4}\right] I_n(\mu)\Big|_{\mu=2z/c}. \tag{54}$$

The preceding expressions can be evaluated and expanded in ascending powers of z, which is effectively an expansion in ascending powers of ζ. The first two correction terms for the short-range expansion of the dipole shift therefore read

$$\hbar^2\mathcal{E}_1(z) = -\frac{\hbar}{32\pi\epsilon_0 z^3}\sum_n\frac{\left|f_{n0}^{(1)}\right|^2}{\omega_{n0}} + \frac{3\hbar}{(4\pi)^2\epsilon_0 z^2 c}\sum_n\left|f_{n0}^{(1)}\right|^2 - \frac{\hbar}{8\pi\epsilon_0 z c^2}\sum_n\left|f_{n0}^{(1)}\right|^2\omega_{n0} + O(z^0). \tag{55}$$

Each of the correction terms involves a sum over oscillator strengths. The quadrupole shift gives rise to the following correction terms:

$$\hbar^2\mathcal{E}_2(z) = -\frac{\hbar}{32\pi\epsilon_0 z^5}\sum_n\frac{\left|f_{n0}^{(2)}\right|^2}{\omega_{n0}} + \frac{3\hbar}{(4\pi)^2\epsilon_0 z^4 c}\sum_n\left|f_{n0}^{(2)}\right|^2 - \frac{\hbar}{192\pi\epsilon_0 z^3 c^2}\sum_n\left|f_{n0}^{(2)}\right|^2\omega_{n0} + O(z^{-2}). \tag{56}$$

For the leading term in each of the preceding expansions, we have, in view of Eq. (50),

$$\sum_n\frac{f_{n0}^{(L)}}{\hbar\omega_{n0}} = \frac{2\hbar}{\pi}\int_0^\infty d\omega\,\alpha_L(\omega), \tag{57}$$

so the leading order terms in Eqs. (55) and (56) agree with the general result (49). For the first correction term, we can use the representation

$$\sum_n f_{n0}^{(L)} = \lim_{\omega\to\infty}(\hbar\omega)^2\alpha_k(\omega). \tag{58}$$

For the dipole case ($L=1$), this can be further simplified to

$$\sum_n f_{n0}^{(1)} = \frac{2e^2}{3}\langle R^i(H-E_0)R^i\rangle = \frac{\hbar^2e^2}{m}N, \tag{59}$$

where N is the number of electrons in the atom, and $R^i = \sum_{k=1}^N r_k^i$ is obtained after summing over all electrons in the atom. For the correction term to the quadrupole interaction, we have

$$\sum_n f_{n0}^{(2)} = \frac{3e^2}{5}\langle r^{ij}(H-E_0)r^{ij}\rangle = 2\frac{(\hbar e)^2}{m}\sum_{k=1}^N\langle r_k^2\rangle, \tag{60}$$

where $R^{ij} = \sum_{k=1}^N(r_k^i r_k^j - \frac{1}{3}\delta^{ij}r_k^2)$. Specifically, we find the following correction terms, respectively, for the dipole and quadrupole shifts:

$$\mathcal{E}_1(z) = -\frac{\hbar}{(4\pi)^2\epsilon_0 z^3}\int_0^\infty d\omega\,\alpha_1(i\omega) + \frac{3\alpha}{4\pi}N\alpha^2mc^2\left(\frac{a_0}{z}\right)^2 + O(z^{-1}), \tag{61a}$$

$$\mathcal{E}_2(z) = -\frac{\hbar}{(4\pi)^2\epsilon_0 z^5}\int_0^\infty d\omega\,\alpha_2(i\omega) + \frac{3\alpha}{2\pi}\alpha^2mc^2\left(\frac{a_0}{z}\right)^4\sum_{k=1}^N\frac{\langle r_k^2\rangle}{a_0^2} + O(z^{-3}), \tag{61b}$$

where a_0 is the Bohr radius. These formulas are generally applicable. Note that the energy scale α^3mc^2, which appears in the correction terms in Eq. (61), is smaller than the energy corresponding to the Rydberg constant by a factor of α (we have $\alpha^3mc^2 = 4\pi\hbar\alpha R_\infty c = 2h\alpha R_\infty c$). The correction term for both the dipole term and the quadrupole term is suppressed with respect to the leading term by a relative factor $\alpha z/a_0 \ll 1$ (because we assume that $z \ll a_0/\alpha$).

V. DIELECTRIC WALL, ARBITRARY RANGE

Let us start the discussion of the case of a dielectric wall with a minireview of available results. The original derivation of Ref. [2] has been reconsidered and cast into a more manageable form by Tikochinsky and Spruch [26], and the result has also been recorded in a particularly clear form in Eq. (15) of Ref. [14]. If we let the dielectric constant $\epsilon(\omega)\to\infty$ in the cited Eq. (15) of Ref. [14], then we reach the result recorded here in Eq. (27). Other treatments of the problem have been given by in Refs. [27,28]. Some more material is also contained in Vol. 8 of the textbook course [13]. The generalization of Eq. (27) to an arbitrary dielectric constant ϵ requires the introduction of a function $H(\epsilon,p)$ and can be written only as a double integral.

In principle, the interaction energy of an atom with a dielectric wall can be computed in the same way as for the case of perfectly conducting one [without the simplifying assumptions in Eqs. (12), (16), and (20)]. The TE- and TM-wave vector potentials are obtained as the sum of the potentials listed in Eqs. (18) and (19), without any further simplifications,

$$\vec{A}_{\vec{k}\lambda}^{\rm TE} = \sqrt{\frac{\hbar c^2}{2\epsilon_0 V}}\vec{\epsilon}_{\vec{k}\lambda}\left(e^{ik_3z} - \frac{k_3-k_3'}{k_3+k_3'}e^{-ik_3z}\right)e^{i\vec{k}_\perp\cdot\vec{r}}, \tag{62a}$$

$$\vec{A}_{\vec{k}\lambda}^{\rm TM} = \sqrt{\frac{\hbar c^2}{2\epsilon_0 V}}\left[\left(\vec{\epsilon}_{\vec{k}\lambda}\times\frac{\vec{k}}{k}\right)\left(e^{2ik_3z} - \frac{\epsilon(\omega)k_3-k_3'}{\epsilon(\omega)k_3+k_3'}\right) \times e^{-ik_3z} + 2\left(\vec{\epsilon}_{\lambda\vec{k}}\times\frac{\vec{k}_\perp}{k}\right)\frac{\epsilon(\omega)k_3-k_3'}{\epsilon(\omega)k_3+k_3'}e^{-ik_3z}\right]e^{i\vec{k}_\perp\cdot\vec{r}}, \tag{62b}$$

which can be inserted into the formula for the energy of an atom in an external field [Eq. (22)]. The result [2] for the dipole

polarizability has been derived in this manner,

$$\mathcal{E}_1(z) = -\frac{\hbar}{2\pi c^3}\frac{1}{4\pi\epsilon_0}\int_0^\infty d\omega\,\omega^3\alpha_1(i\omega) \times \int_1^\infty d\xi\, e^{-2\xi\omega z/c}\mathrm{H}(\xi,\epsilon(i\omega)), \tag{63a}$$

where

$$\mathrm{H}(\xi,\epsilon) = (1-2\xi^2)\frac{\sqrt{\xi^2+\epsilon-1}-\epsilon\xi}{\sqrt{\xi^2+\epsilon-1}+\epsilon\xi} + \frac{\sqrt{\xi^2+\epsilon-1}-\xi}{\sqrt{\xi^2+\epsilon-1}+\xi}. \tag{63b}$$

This result can be approximated, for $z \to 0$, with the help of the following integral:

$$\int_1^\infty d\xi\, e^{-2\xi\omega z/c}\mathrm{H}(\xi,\epsilon) = \frac{1}{2}\left(\frac{c}{z\omega}\right)^3\frac{\epsilon-1}{\epsilon+1} + \frac{1}{2}\left(\frac{c}{z\omega}\right)\frac{(\epsilon-1)(3\epsilon+1)}{(\epsilon+1)^2} + O(z^0). \tag{64}$$

Inserting (64) into (63), we have

$$\mathcal{E}_1(z) \overset{z\to 0}{=} -\frac{\hbar}{(4\pi)^2\epsilon_0 z^3}\int_0^\infty d\omega\,\alpha_1(i\omega)\frac{\epsilon(i\omega)-1}{\epsilon(i\omega)+1}, \tag{65}$$

in full agreement with (28) for the limit of a perfect conductor, $\epsilon(\mathrm{i}\omega) \to \infty$.

In order to derive an analogous expression for the case of quadrupole polarizability, gradients of electromagnetic potentials need to be computed. Using the expression (30) for the energy of a quadrupole polarizable particle and using the same procedure as for the case of atom-conductor interaction we obtain

$$\mathcal{E}_2(z) = -\frac{\hbar}{12\pi c^5}\frac{1}{4\pi\epsilon_0}\int_0^\infty d\omega\,\omega^5\alpha_2(i\omega) \times \int_1^\infty d\xi\, e^{-2\xi\omega z/c}(2\xi^2-1)\mathrm{H}(\xi,\epsilon(i\omega)). \tag{66}$$

In the perfect conductor limit ($\epsilon \to \infty$), the preceding formula reduces to the previously derived result in Eq. (32). Moreover, in the limit of small distances (or in the limit of $c \to \infty$) the preceding formula reproduces the short-range asymptotic result of Ref. [17], which was derived for an arbitrary dielectric constant and which reads

$$\mathcal{E}_2(z) \overset{z\to 0}{=} -\frac{\hbar}{(4\pi)^2\epsilon_0 z^5}\int_0^\infty d\omega\,\alpha_2(i\omega)\frac{\epsilon(i\omega)-1}{\epsilon(i\omega)+1}. \tag{67}$$

Using computer algebra [18], it is a lengthy but manageable exercise to calculate the octupole and hexadecupole energy shifts,

$$\mathcal{E}_3(z) = -\frac{\hbar}{180\pi c^7}\frac{1}{4\pi\epsilon_0}\int_0^\infty d\omega\,\omega^7\alpha_3(i\omega)\int_1^\infty d\xi\, e^{-2\xi\omega z/c} \times (4\xi^4-4\xi^2+1)\mathrm{H}(\xi,\epsilon(\mathrm{i}\omega)), \tag{68}$$

and

$$\mathcal{E}_4(z) = -\frac{\hbar}{5040\pi c^9}\frac{1}{4\pi\epsilon_0}\int_0^\infty d\omega\,\omega^9\alpha_4(i\omega)\int_1^\infty d\xi\, e^{-2\xi\omega z/c} \times (8\xi^6-12\xi^4+6\xi^2-1)\mathrm{H}(\xi,\epsilon(i\omega)). \tag{69}$$

TABLE I. Coefficients for the first few resonances for α-quartz according to the fitting formula (70) (ordinary optical axis). The ω_k and γ_k are measured in atomic units, that is, in units of $\alpha^2mc^2 = 4\pi\hbar R_\infty c$, where R_∞ is the Rydberg constant.

k	α_k	ω_k	γ_k
	Vibrational excitations		
1	$1.042\,74 \times 10^{-2}$	$1.826\,71 \times 10^{-3}$	$1.290\,01 \times 10^{-5}$
2	$8.527\,62 \times 10^{-2}$	$2.218\,25 \times 10^{-3}$	$1.832\,57 \times 10^{-5}$
3	$0.156\,98 \times 10^{-2}$	$3.181\,00 \times 10^{-3}$	$3.159\,99 \times 10^{-5}$
4	$1.064\,16 \times 10^{-2}$	$3.668\,24 \times 10^{-3}$	$3.195\,71 \times 10^{-5}$
5	$5.516\,23 \times 10^{-2}$	$5.234\,01 \times 10^{-3}$	$3.606\,49 \times 10^{-5}$
6	$4.553\,89 \times 10^{-2}$	$5.342\,06 \times 10^{-3}$	$3.890\,10 \times 10^{-5}$
	Interband excitations		
7	$1.053\,01 \times 10^{-2}$	$3.890\,05 \times 10^{-1}$	$1.117\,67 \times 10^{-2}$
8	$4.712\,12 \times 10^{-2}$	$4.451\,02 \times 10^{-1}$	$5.283\,24 \times 10^{-2}$
9	$4.978\,63 \times 10^{-2}$	$5.373\,78 \times 10^{-1}$	$7.324\,83 \times 10^{-2}$
10	$1.057\,75 \times 10^{-1}$	$6.580\,90 \times 10^{-1}$	$1.300\,09 \times 10^{-1}$
11	$1.115\,86 \times 10^{-1}$	$8.259\,62 \times 10^{-1}$	$2.401\,49 \times 10^{-1}$

VI. He–α-QUARTZ INTERACTION

In order to analyze the interaction of a helium atom with a dielectric wall, we have to model the surface properties accurately. We have thus scanned the extensive tabulated data from the reference volume [29] via an optical character-recognition software. A fit to these experimental data for the real and imaginary part of the dielectric constant $\epsilon(\omega) = n(\omega) + ik(\omega)$ with an analytic function of the frequency then leads to a satisfactory representation of the dielectric constant for all frequencies. The following functional form was found to lead to a satisfactory fit of the available data (see Tables I and II):

$$\rho(\omega) = \frac{\epsilon(\omega)-1}{\epsilon(\omega)+2} = \frac{[n(\omega)+ik(\omega)]^2-1}{[n(\omega)+ik(\omega)]^2+2} \simeq \sum_{k=1}^{n}\frac{\alpha_k}{\omega_k^2 - \mathrm{i}\gamma_k\omega - \omega^2}. \tag{70}$$

TABLE II. Same as Table I for the extraordinary axis.

k	α_k	ω_k	γ_k
	Vibrational excitations		
1	$3.633\,44 \times 10^{-2}$	$1.736\,67 \times 10^{-3}$	$2.319\,16 \times 10^{-5}$
2	$0.084\,45 \times 10^{-2}$	$2.313\,39 \times 10^{-3}$	$1.517\,16 \times 10^{-5}$
3	$7.540\,27 \times 10^{-2}$	$2.420\,18 \times 10^{-3}$	$2.999\,94 \times 10^{-5}$
4	$1.080\,98 \times 10^{-2}$	$3.578\,86 \times 10^{-3}$	$3.494\,81 \times 10^{-5}$
5	$1.028\,81 \times 10^{-1}$	$5.309\,09 \times 10^{-3}$	$4.464\,37 \times 10^{-5}$
	Interband excitations		
6	$1.053\,01 \times 10^{-2}$	$3.890\,05 \times 10^{-1}$	$1.117\,67 \times 10^{-2}$
7	$4.712\,12 \times 10^{-2}$	$4.451\,02 \times 10^{-1}$	$5.283\,24 \times 10^{-2}$
8	$4.978\,63 \times 10^{-2}$	$5.373\,78 \times 10^{-1}$	$7.324\,83 \times 10^{-2}$
9	$1.057\,75 \times 10^{-1}$	$6.580\,90 \times 10^{-1}$	$1.300\,09 \times 10^{-2}$
10	$1.115\,86 \times 10^{-1}$	$8.259\,62 \times 10^{-1}$	$2.401\,49 \times 10^{-2}$

The original dielectric response function $[\epsilon(\omega)-1]/[\epsilon(\omega)+1]$ can be reproduced as follows:

$$\frac{\epsilon(\omega)-1}{\epsilon(\omega)+1}=\frac{3\rho(\omega)}{\rho(\omega)+2}. \tag{71}$$

This fitting procedure leads to a very good representation of the data for both infrared and ultraviolet absorption bands. We then employ the Kramers-Kronig relation for the dielectric constant ϵ as a function of the frequency, in order to obtain $\epsilon(i\omega)$ along the imaginary axis. Note that this quantity is needed as input for the double integrals in Eqs. (63), (66), (68), and (69).

We then calculate accurately the dipole, quadrupole, and octupole dynamic polarizabilities of helium. An evaluation of the double integrals in the aforementioned formulas then gives the potential at a given distance from the wall. Inspired by the considerations in Sec. IV A, we then fit the obtained data for the distance-dependent interaction potential of 2^L multipole order with the functional form

$$\mathcal{E}_L(z)=-\frac{C_{2L+1}}{z^{2L+1}}f_{2L+1}\left(\frac{\alpha^2 mcz}{\hbar}\right)=-\frac{C_{2L+1}}{z^{2L+1}}f_{2L+1}(\zeta), \tag{72}$$

where ζ is defined in Eq. (47). In atomic units, the function f would be given in terms of the variable $f=f(\alpha z)$. A convenient model is

$$f_{2L+1}(\zeta)=\frac{1+a_1\zeta+a_2\zeta^2+a_3\zeta^3}{1+a_1\zeta+b_2\zeta^2+b_3\zeta^3+b_4\zeta^4}. \tag{73}$$

We choose the linear term $a_1\zeta$ in the denominator to be equal to the linear term in the numerator, so that the modification of f for small ζ is of relative order ζ^2. The [3/4] Padé approximant (73) is conceptually simple but sufficiently adjustable to capture details of the potential. The ultraviolet divergence, which otherwise leads to a correction term of relative order ζ, remains suppressed for a realistic dielectric, and this aspect provides additional justification for the chosen functional form. The rational function constitutes a generalization of the concept of the z_0 parameter put forth in Ref. [24].

A numerical evaluation of the formulas (63), (66), and (67) for the ground-state of hydrogen and helium atoms then proceeds using polarizabilities at purely imaginary frequencies (obtained using a variational method). The results for the asymptotic constants thus obtained are summarized in Table III. The C_{2L+1} constants in the first column are in full agreement with known analytic formulas for a hydrogen atom interacting with a perfect conductor. Note that these constants only determine the leading coefficients in the small-distance asymptotics for the specific multipole components of order 2^L and that they do not say anything about arbitrary distances. To this end, we also present sample values of the dimensionless van der Waals retardation functions f_{2L+1} in Tables IV and V and the coefficients used for the construction of the Padé approximants in Table VI. From the graphical representations in Figs. 1 and 2, it is clear that a simple $f_3(\zeta)=\frac{a}{a+z}$, which would correspond to a [0/1] Padé approximant, cannot lead to a satisfactory representation of the numerical data for the van der Waals retardation function, as evident from the double-hump structure plotted in Fig. 2. A more complex form like Eq. (73) is definitely required. The two separate humps in Figs. 1 and 2 are due to the vibrational and interband excitations of α-quartz, which are clearly distinguished by their frequency ranges (see Tables I and II). The interband transitions contribute significantly to the interaction potential for small distances, whereas the low-frequency vibrational excitations contribute to the large-distance behavior.

TABLE III. Asymptotic constants in dipole, quadrupole, and octupole components of the energy of helium and hydrogen atoms interacting with a perfect conductor and with α-quartz. The results are given in atomic units. In SI units, the asymptotic energy shift for hydrogen is obtained as $\mathcal{E}_L(z)=-C_{2L+1}\alpha^2 mc^2(a_0/z)^{2L+1}$, where a_0 is the Bohr radius and C_{2L+1} is the dimensionless numerical constant given in the table.

	H ($1^1S_{1/2}$)		He (1^1S_0)	
	$\epsilon=\infty$	α-Quartz	$\epsilon=\infty$	α-Quartz
C_3	0.250	0.060	0.188	0.033
C_5	1.125	0.172	0.396	0.062
C_7	11.250	2.505	1.877	0.282

TABLE IV. Sample values of the functions $f_3(z)$, defined as ratios between the dipole part of the atom-surface interaction and its short-distance asymptotics [see Eq. (72)]. The distance z is measured in atomic units (a.u.), that is, in units of the Bohr radius a_0.

	H ($1^1S_{1/2}$)		He (1^1S_0)	
z (units in a_0)	$\epsilon=\infty$	α-Quartz	$\epsilon=\infty$	α-Quartz
0	1.000	1.000	1.000	1.000
10	0.977	0.997	0.941	0.992
20	0.955	0.989	0.887	0.976
50	0.892	0.955	0.756	0.914
100	0.802	0.889	0.604	0.808
200	0.663	0.763	0.425	0.640
500	0.426	0.515	0.217	0.377
1000	0.259	0.322	0.117	0.217
2000	0.141	0.180	0.060	0.116
5000	0.058	0.078	0.024	0.377
10 000	0.029	0.042	0.012	0.026

TABLE V. Sample values of the van der Waals retardation functions $f_n(z)$ for the He-SiO_2 interaction.

z (units in a_0)	$f_3(\alpha z)$	$f_5(\alpha z)$	$f_7(\alpha z)$
0	1.000	1.000	1.000
10	0.992	0.997	0.998
20	0.976	0.989	0.993
50	0.914	0.952	0.966
100	0.808	0.875	0.906
200	0.640	0.732	0.781
500	0.377	0.465	0.522
1000	0.217	0.278	0.322
2000	0.116	0.151	0.178
5000	0.377	0.064	0.076
10 000	0.026	0.034	0.040

TABLE VI. Coefficients for the construction of the Padé approximation to the retardation functions $f_3(\zeta)$, $f_5(\zeta)$, and $f_7(\zeta)$. Because the coefficients have inverse powers of distance as their physical dimension, we again stress that $\zeta = \alpha z$ where z is measured in atomic units.

	$f_3(\zeta)$	$f_5(\zeta)$	$f_7(\zeta)$
a_1	4.551×10^{0}	2.333×10^{0}	1.677×10^{0}
a_2	8.302×10^{-1}	3.382×10^{-1}	2.053×10^{-1}
a_3	6.223×10^{-3}	1.818×10^{-3}	8.999×10^{-4}
b_2	2.606×10^{0}	1.003×10^{0}	6.044×10^{-1}
b_3	4.956×10^{-1}	1.519×10^{-1}	7.717×10^{-2}
b_4	2.393×10^{-3}	5.252×10^{-4}	2.177×10^{-4}

In order to validate our analytic model for the dielectric constant of SiO_2 we have computed the C_3 coefficient for the interaction of positronium with the α-quartz surface for which independent theoretical values have been published [30,31]. Our result of 8.22 eV a_0^3 is in satisfactory agreement with the result of 8.43 eV a_0^3 reported in Refs. [30,31], with a difference of less than 3% in the numerical results. We take the opportunity to discuss the theoretical uncertainty of the numerical values reported in Tables I–VI of this article.

In Tables I and II, the fit parameters entering Eq. (70) are given with an accuracy of six decimal digits. We estimate the accuracy of the fitting function given in Eq. (70) to be on the order of 5%, uniformly over the entire range of frequencies ω required for the current study. However, we give the fitting parameters in Tables I and II with higher accuracy, because the actual value of the fitting function $\rho(\omega)$, which has pronounced peaks, depends very sensitively on the parameters used in the fit. In Tables III–V, numerical values for coefficients C_3, C_5, and C_7, and for the van der Waals retardation functions f_3, f_5, and f_7 are provided. With the exception of the values given for H in the first column of Table III, which are exact, we estimate the numerical uncertainty of these values not to exceed 5%. In Table VI, fit parameters are given for the (smooth) van der Waals retardation functions f_3, f_5, and f_7. Here, too, we estimate the accuracy of the fitted function given in Eq. (73) to be on the order of 5%. Because the fitting functions given by (73) are smooth, it is not necessary to give the fit parameters with higher accuracy in this particular case.

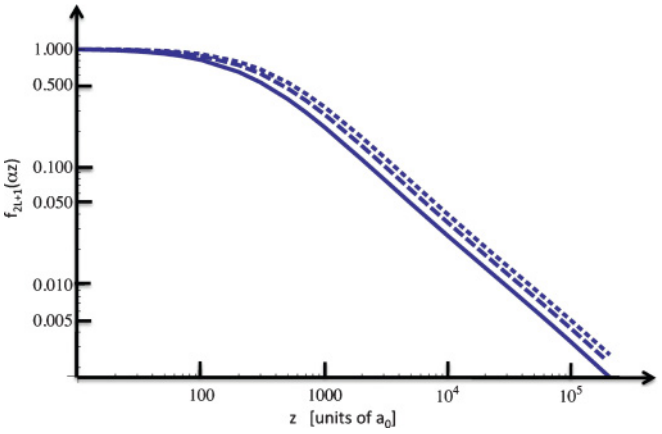

FIG. 1. (Color online) Double-logarithmic plot of the van der Waals retardation functions $f_3(\alpha z) = -z^3\mathcal{E}_1(z)/C_3$ (solid line), $f_5(\alpha z) = -z^5\mathcal{E}_2(z)/C_5$ (long-dashed line), and $f_7(\alpha z) = -z^7\mathcal{E}_3(z)/C_7$ (short dashed) in the range $z \in (10, 10^5)$ for the He–α-quartz interaction. These are related to the dipole, quadrupole and octupole interactions, respectively. The linear asymptotics for large z implies that the leading power for large z of $f_{2L+1}(z)$ is proportional to z^{-1}, as it should be. Note that z is given in atomic units, that is, in units of the Bohr radius a_0. One sees that as $z \to 0$, $f(z)$ approaches unity.

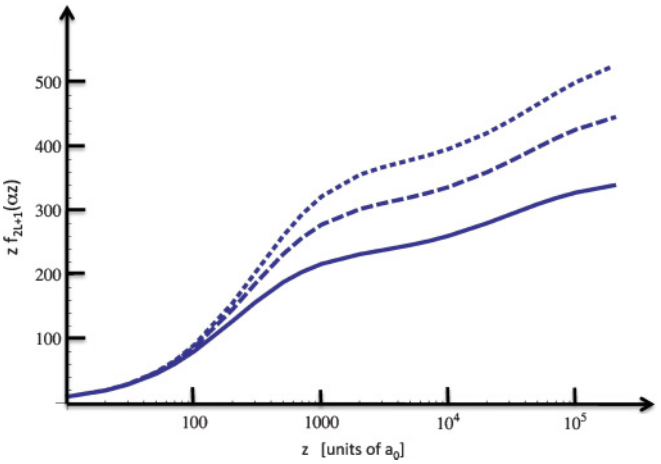

FIG. 2. (Color online) Plot of the function $zf_3(\alpha z)$ (solid line), $zf_5(\alpha z)$ (long-dashed line), and $zf_7(\alpha z)$ (short dashes) in the range $z \in (10, 10^5)$ for the He–α-quartz interaction. These are related to the dipole, quadrupole, and octupole effects, respectively. A logarithmic scale is used for the z coordinate. For $z \to \infty$, all plotted graphs approach a constant. There are two humps for small ($10^3 a_0$) and large distances ($10^5 a_0$, i.e., few microns). These result from two absorption regions: interband transitions in the ultraviolet region and isolated absorption peaks in the infrared. These are relevant to small and large distances from the wall, respectively.

VII. CONCLUSIONS

The purpose of this article has been to advance our understanding of long-range interactions of atoms with conductors, and with dielectric walls, via a combination of analytic considerations and numerical calculations. As clarified in Sec. IV A, the multipole expansion is an expansion of the atom-wall interaction in powers of (a_0/z), where a_0 is the Bohr radius and z is the atom-wall distance. This expansion thus is always valid for any reasonable application of the long-range theory. However, the importance of the multipole effects grows as we approach the wall and z becomes smaller. The higher-order corrections are well represented by a rational function of the variable $\alpha z/a_0 = z/\lambda\!\!\!^{-}_0$, where α is the fine-structure constant and $\lambda\!\!\!^{-}_0$ is the wavelength (divided by 2π) of a typical atomic transition, $\lambda\!\!\!^{-}_0 = \hbar/(\alpha^2 mc)$. This second scale is larger than the Bohr radius by a factor $\alpha^{-1} \approx 137.036$. We find that each term in the multipole expansion, in turn, is multiplied by a rational function of the latter parameter $z/\lambda\!\!\!^{-}_0$, which can be larger or smaller than unity depending on the atom-wall distance [see Eqs. (43), (45), and (73)].

There have been certain gaps in the literature concerning the treatment of multipole corrections, even for perfectly

conducting walls. We have attempted to clarify how the multipole interactions of atoms with surfaces (atom-wall interactions) should be treated for an arbitrary distance z of the atom and the macroscopic structure (see Sec. III). Interpolating formulas are found which clarify how the transition from the $1/z^{2L+2}$ long-range interaction to the $1/z^{2L+1}$ short-range interaction proceeds for the multipole of order 2^L.

We have also attempted to clarify how the asymptotic expansions of the atom-wall potentials have to be interpreted physically (see Sec. IV). A certain "anomaly" in the asymptotic expansion for small distances, which occurs only in the case of a perfect conductor, has been uncovered (Sec. IV B). This "anomaly" leads to the appearance of a linear (rather than quadratic) correction term for the dipole and quadrupole interaction energies in terms of the parameter $z/\lambda\!\!\!^{-}_0$. Rather general formulas are found for the linear correction term.

We have also generalized the results to the interaction of an arbitrary ground-state atom interacting with a dielectric wall for all multipoles up to the hexadecupole interaction (Sec. V), with full allowance for retardation and with full account of the dielectric response function of the medium. We then demonstrate the utility of the results for practical purposes, by addressing the interaction of helium with α-quartz (Sec. VI). Our analysis relies heavily on an accurate and appropriate representation of all data available today for the dielectric response function of realistic materials [29], and on an analytic continuation thereof to imaginary probe frequencies. For the interaction with perfect conductors, a few results for asymptotic coefficients are reproduced using our formalism (see Table III), and more results are obtained for the interaction with α-quartz. We find that, surprisingly, the vibrational and interband excitations play very distinctive roles at different ranges of the atom-wall interaction (see Figs. 1 and 2).

As an incentive for future work, we can say that we do not consider here mixing terms between different multipole components as, for example, the dipole-octupole mixing terms which have already been mentioned in Ref. [32], in a different context, namely, for the long-range atom-atom interaction. In that sense, our results for the expansions in powers of a_0/z even have to be considered as incomplete. However, they give a good quantitative estimate for the corrections that have to be expected if higher multipoles are taken into account, and they pave the way for a future systematic investigation of the higher-order effects. Moreover, relativistic corrections to the atom-wall interaction of relative order α^2 have also been neglected in the current analysis. These provide further room for an improvement of our understanding of the interactions that are mediated by virtual excitations of the quantum fields. However, as shown in Sec. VII, the quantitative predictions of theory also depend crucially on an accurate representation of available data for the dielectric response function, which needs to be cast into a manageable analytic form. Even with the simplifications described in Sec. VII, the determination of enough points for the reliable calculation of the rational coefficients in Table VI took several days in a massively parallel computing environment, because for each distance, a double integral involving both the dielectric response function of the medium and the polarizability of the atom needs to be evaluated.

ACKNOWLEDGMENTS

This project was supported by the National Science Foundation (Grant PHY-8555454) and by a precision measurement grant from the National Institute of Standards and Technology. G.L. acknowledges support by the Deutsche Forschungsgemeinschaft (DFG, contract Je285/5-1).

[1] H. B. G. Casimir and D. Polder, Phys. Rev. **73**, 360 (1948).
[2] E. M. Lifshitz, Zh. Eksp. Teor. Fiz. **29**, 94 (1955) [JETP **2**, 73 (1956)].
[3] M. De Kieviet, D. Dubbers, C. Schmidt, and M. Skrzipczyk, Phys. Rev. Lett. **75**, 1919 (1995).
[4] M. De Kieviet, D. Dubbers, M. Klein, U. Pieles, and M. Skrzipczyk, Surf. Sci. **377**, 1112 (1997).
[5] V. Druzhinina and M. DeKieviet, Phys. Rev. Lett. **91**, 193202 (2003).
[6] G. Łach, M. DeKieviet, and U. D. Jentschura, Int. J. Mod. Phys. A (to be published).
[7] P. J. Mohr, B. N. Taylor, and D. B. Newell, Rev. Mod. Phys. **80**, 633 (2008).
[8] Z. C. Yan, J. F. Babb, A. Dalgarno, and G. W. F. Drake, Phys. Rev. A **54**, 2824 (1996).
[9] K. Pachucki, Phys. Rev. A **71**, 012503 (2005).
[10] P. W. Milonni, *The Quantum Vacuum* (Academic Press, San Diego, 1994).
[11] W. Demtröder, *Laserspektroskopie*, 3rd ed. (Springer, Berlin, 1993).
[12] J. D. Jackson, *Classical Electrodynamics*, 3rd ed. (J. Wiley & Sons, New York, 1998).
[13] L. D. Landau and E. M. Lifshitz, *Electrodynamics of Continuous Media* (Pergamon Press, Oxford, UK, 1960).
[14] Z. C. Yan, A. Dalgarno, and J. F. Babb, Phys. Rev. A **55**, 2882 (1997).
[15] X. P. Jiang, F. Toigo, and M. W. Cole, Surf. Sci. **145**, 281 (1984).
[16] X. P. Jiang, F. Toigo, and M. W. Cole, Surf. Sci. **148**, 21 (1984).
[17] J. M. Hutson, P. W. Fowler, and E. Zaremba, Surf. Sci. **175**, L775 (1986).
[18] S. Wolfram, *Mathematica—A System for Doing Mathematics by Computer* (Addison-Wesley, Reading, MA, 1988).
[19] M. J. Mehl and W. L. Schaich, Phys. Rev. A **16**, 921 (1977).
[20] M. J. Mehl and W. L. Schaich, Phys. Rev. A **21**, 1177 (1980).
[21] Y. Liu and W. A. Goddard, Mater. Trans. **50**, 1664 (2009).
[22] A. M. Marvin and F. Toigo, Phys. Rev. A **25**, 782 (1982).
[23] A. M. Marvin and F. Toigo, Phys. Rev. A **25**, 803 (1982).
[24] A. Liebsch, Phys. Rev. B **35**, 9030 (1987).
[25] M. Abramowitz and I. A. Stegun, *Handbook of Mathematical Functions*, 10th ed. (National Bureau of Standards, Washington, DC, 1972).

[26] Y. Tikochinsky and L. Spruch, Phys. Rev. A **48**, 4223 (1993).
[27] I. E. Dzyaloshinskii, E. M. Lifshitz, and L. P. Pitaevskii, Adv. Phys. **29**, 165 (1961).
[28] V. A. Parsegian, Mol. Phys. **27**, 1503 (1974).
[29] E. D. Palik, *Handbook of Optical Constants of Solids* (Academic Press, San Diego, 1985).
[30] R. Saniz, B. Barbiellini, P. M. Platzman, and A. J. Freeman, Phys. Rev. Lett. **99**, 096101 (2007).
[31] R. Saniz, B. Barbiellini, P. M. Platzman, and A. J. Freeman, Phys. Rev. Lett. **100**, 019902 (2008).
[32] S. Ray, J. D. Lyons, and T. P. Das, Phys. Rev. A **174**, 104 (1968).